

FLUID–DYNAMIC MODEL EQUATIONS FOR A GAS WITH SLOW REVERSIBLE BIMOLECULAR REACTIONS*

MARIA GROPPI[†], ALBERTO ROSSANI[‡], AND GIAMPIERO SPIGA[§]

Abstract. The dispersion relation and shock structure of a gas mixture undergoing a bimolecular chemical reaction are studied by means of a hydrodynamic model deduced from the relevant kinetic equations. Qualitative changes in the solution, in particular loss of smoothness, for varying parameters (including Mach number and strength of the chemical reaction rate) are investigated, and numerical results are presented. In the limits of vanishing or diverging reactive relaxation times the “equilibrium” and “frozen” thermodynamical situations are recovered.

Key words. Reactive gas mixtures, shock wave structure, dispersion relation, hydrodynamic limits.

AMS subject classifications. 82C40, 76V05, 76A02, 76L05.

1. Introduction

Bimolecular chemical reactions in dilute gaseous systems may be rigorously studied on the basis of kinetic theory in terms of Boltzmann-like integro-differential nonlinear equations [4, 10, 18]. One of the main motivations of a kinetic approach is the need for a rigorous derivation of hydrodynamic equations for the macroscopic fields to be used in real world applications. At the same time, kinetic equations [8, 13] or their relaxation time approximations [14, 17] are being used for investigating classical fundamental issues of Fluid Dynamics, like evaporation-condensation, wave propagation, shock structure, Riemann problem, extending them from the inert [9, 16, 21, 22] to the reactive frame [2, 11]. In this paper we shall deal with such questions by thoroughly exploiting an hydrodynamic closure following from a simple kinetic model proposed some years ago by some of the authors [20], and later enlarged and improved (see [3] for a review). The model could account for internal (molecular) energy states, but they will be ignored here for technical simplicity. The closure is relevant to a situation close to thermal equilibrium in the case of a slow chemical reaction, so that mechanical collisions are the dominant process driving the evolution. These fluid-dynamic-type equations have already been used in the analysis of reactive mixtures [7, 12], and in particular in the determination of traveling wave solutions [6, 19]. Here we intend to make the analysis systematic, with particular emphasis on the dispersion relation and shock wave structure, in order to cover all possible ranges of the main physical parameters, mainly the chemical collision frequency (or relaxation time) and the Mach number, with reference to the limiting situations of extremely slow reactions (inert mixture, frozen system), or of extremely fast reactions (chemical relaxation as fast as the mechanical one, equilibrium system) [5, 23]. Analytical investigation, based on simple qualitative methods from the theory of dynamical systems, as well as numerical results, indicate the presence of damping in all intermediate cases between

*Received: October 7, 2008; accepted (in revised version): December 9, 2008. Communicated by Lorenzo Pareschi.

[†]Dipartimento di Matematica, Università di Parma, Viale G. P. Usberti 53/A - 43100 Parma, Italy (maria.groppi@unipr.it).

[‡]Dipartimento di Matematica & Istituto Nazionale di Fisica della Materia, Politecnico di Torino, Corso Duca degli Abruzzi 24 - 10129 Torino, Italy (alberto.rossani@polito.it).

[§]Dipartimento di Matematica, Università di Parma, Viale G. P. Usberti 53/A - 43100 Parma, Italy (giampiero.spiga@unipr.it). Corresponding author.

the undamped inert and fast limits, as well as existence and uniqueness of a shock solution for any admissible Mach number. The shock profile is smooth in a proper range of slightly supersonic flows, but then loses regularity for increasing Mach number, leaving only a weak solution with a well defined jump. The present results may be considered as a necessary comparison test in view of a deeper kinetic analysis, and also as a generalization to a problem with several dependent variables, consistently deduced from kinetic equations, of classical results which are known to be valid for simpler heuristic thermodynamical models [5, 24]. Indeed, to our knowledge, the only reactive system for which significant results of this kind are explicitly known, from thermodynamical considerations, is the so called (two-species) dissociating gas, in which an acoustic equation may be established and the frozen and equilibrium sound speeds have been determined, going through the analysis of the degree of dissociation and of the relevant law of mass action [23].

We recall here for convenience the main properties of kinetic equations for a four component gas mixture of species A^i , $i=1,\dots,4$, with masses m^i and energies of chemical link E^i , colliding among themselves and undergoing the reversible bimolecular chemical reaction



according to the model proposed in [20] for monoatomic gases and later extended to molecules with internal structure in [13]. For the sake of simplicity, here we will focus only on the former paper in order to point out the most essential features introduced by chemistry, thus ignoring the non-translational degrees of freedom which clearly play some role in realistic reactions. We will conventionally assume the direct reaction in (1.1) as endothermic, namely

$$\Delta E = - \sum_{i=1}^4 \Lambda^i E^i = E^3 + E^4 - E^1 - E^2 > 0, \quad (1.2)$$

where Λ^i is a component of the string of the stoichiometric coefficients $(1, 1, -1, -1)$.

Collision invariants correspond to conservation of momentum and total (kinetic plus chemical) energy, and to conservation of particles in the independent pairs of species $(1, 3)$, $(1, 4)$, $(2, 4)$ (proper linear combinations reproduce conservation of total particle number and of total mass).

Since an extended version of Boltzmann's H -theorem holds, collision equilibria are determined as a family of local Maxwellians at a common mass velocity \mathbf{u} and temperature T , with number densities n^i related by the mass action law

$$\frac{n^1 n^2}{n^3 n^4} = \frac{\chi^1 \chi^2}{\chi^3 \chi^4} = \left(\frac{m^1 m^2}{m^3 m^4} \right)^{3/2} \exp\left(\frac{\Delta E}{KT} \right), \quad (1.3)$$

expressing chemical equilibrium between direct and inverse reaction rates at temperature T . In (1.3) we have introduced the concentration fractions

$$\chi^i = \frac{n^i}{n}, \quad \sum_{i=1}^4 \chi^i = 1. \quad (1.4)$$

The simplest closure of the exact conservation equations is provided as usual by a zero-order approximation around equilibrium and yields the reactive Euler equations, a homogeneous system of hyperbolic partial differential equations which must be

coupled with the mass action law (1.3) to provide a closed set of differential-algebraic equations for the unknown fields n^i, \mathbf{u}, T [13]. The same unknowns would have to be determined if the reaction were switched off (inert mixture); in this case collision equilibria would be Maxwellians with all free parameters and the zero-order closure would yield the standard (non-reactive) Euler equations.

The paper is organized as follows. The hydrodynamic model and its connections with kinetic theory, from which it originates, are presented in section 2, where also the limiting situations, frozen and equilibrium, and their relevant results are recalled. The dispersion relation is analyzed in section 3, investigating the time eigenvalue versus the wave number for different parameters and proving universal existence of a complex conjugate pair, which always implies damped propagation modes, as expected. Section 4 is devoted to the investigation of shock wave structure, resorting to recent results on the pertinent reactive Rankine-Hugoniot relations and entropy condition [15]. In particular, the bifurcation value for the Mach number yielding transition from a strong to a weak solution is determined in connection with the associated inert shock problem. Finally, numerical results from the integration of the governing nonlinear differential equations are presented and discussed in section 5, showing the shock profile for varying collision models, upstream conditions, and Mach numbers.

2. Hydrodynamic model equations

When the physical process is dominated by mechanical interactions, in the sense that the typical elastic collision time is much shorter than both chemical collision time and macroscopic scale, nondimensionalization of the reactive Boltzmann equations (a typical procedure of kinetic theory) leads to the appearance of a small dimensionless parameter (essentially, the Knudsen number), whose inverse multiplies the scattering collision integral. This quantifies the dominance of mechanical encounters in leading the whole evolution, and allows a standard asymptotic analysis with respect to the small parameter. This yields, in the asymptotic limit, hydrodynamic equations for the main macroscopic fields, and in particular, to zero-order approximation, the reactive fluid-dynamics equations that we shall be dealing with in the following. We refer to the quoted bibliography for all technical details on the matter, and we only recall here that hydrodynamic quantities are the macroscopic fields associated to the collision invariants of the dominant evolution operator, and may be chosen as the four number densities, the scalar components of velocity, and the gas temperature. Of course, such quantities are not (all) conserved by the chemical collision operators, so that reactive contributions do actually appear in these hydrodynamic equations, making them a set of balance equations, rather than of conservation equations as would occur in the standard case of a non-reacting mixture. Once a specific reaction is chosen, the energy gap ΔE is not a free parameter and spontaneously provides the proper energy unit, so that it disappears completely from the dimensionless equations. However, in order to keep this important quantity explicitly shown in the analytical treatment below, we shall let energy unit be arbitrary (and measure ΔE in that unit). Keeping the same symbols for all nondimensionalized quantities, the reactive macroscopic balance equations to be studied, in one space dimension, read as

$$\begin{aligned} \frac{\partial}{\partial t}(n^i) + \frac{\partial}{\partial x}(n^i u) &= \Lambda^i Q & i = 1, 2, 3, 4 \\ \frac{\partial}{\partial t}(\rho u) + \frac{\partial}{\partial x}(\rho u^2 + nT) &= 0 \end{aligned}$$

$$\frac{\partial}{\partial t} \left(\frac{1}{2} \rho u^2 + \frac{3}{2} nT + \sum_{i=1}^4 E^i n^i \right) + \frac{\partial}{\partial x} \left(\frac{1}{2} \rho u^3 + \frac{5}{2} nT u + \sum_{i=1}^4 E^i n^i u \right) = 0, \quad (2.1)$$

where

$$Q = Q(n^1, n^2, n^3, n^4, T) = \nu_{34}^{12}(T) n^3 n^4 - \nu_{12}^{34}(T) n^1 n^2 \quad (2.2)$$

represents the chemical production term for reactants, and Λ^i are the previously defined stoichiometric coefficients, which appear also in (1.2). The collision frequencies ν_{ij}^{hk} follow from the microscopic knowledge of the corresponding reactive differential cross sections σ_{ij}^{hk} as [3, 20]

$$\nu_{ij}^{hk}(T) = \frac{(m^i m^j)^{3/2}}{(2\pi T)^3} \iiint g \sigma_{ij}^{hk}(g, \psi) \exp \left[-\frac{m^i v^2 + m^j w^2}{2T} \right] d_3 \mathbf{v} d_3 \mathbf{w} d_2 \mathbf{n}, \quad (2.3)$$

where $\mathbf{g} = \mathbf{v} - \mathbf{w}$, $g = |\mathbf{g}|$, and $\cos \psi = \mathbf{n} \cdot \mathbf{g}/g$. By the microreversibility principle, they must be related by the Arrhenius law

$$\nu_{34}^{12}(T) = \left(\frac{m^1 m^2}{m^3 m^4} \right)^{3/2} \exp \left(\frac{\Delta E}{T} \right) \nu_{12}^{34}(T). \quad (2.4)$$

The collision frequencies ν_{ij}^{hk} can be cast in explicit analytical form in correspondence with the most common microscopic collision models. For instance, a simple and general enough collision model, which mimics in some sense the inverse-power-intermolecular-potentials of Rarefied Gas Dynamics [4], could be

$$\sigma_{34}^{12}(g, \psi) = \beta g^{s-1} H \left[g^2 - \frac{2(m^3 + m^4)A}{m^3 m^4} \right] \gamma(\psi), \quad \int \gamma(\psi) d_2 \mathbf{n} = 1, \quad (2.5)$$

where the constant $\beta > 0$ measures the strength of reaction rate, and the real parameter s is positive or negative in correspondence to strong or soft potentials (classical models of Maxwellian molecules and hard spheres are reproduced by $s=0$ and $s=1$, respectively). In addition, H stands for the Heaviside function, and $A > 0$ denotes the (dimensionless) activation energy, the potential barrier that must be overcome even in the exothermic reaction in order to trigger the change of species. The exothermic collision frequency following from option (2.5) is

$$\nu_{34}^{12}(T) = \beta \left(\frac{2(m^3 + m^4)T}{m^3 m^4} \right)^{s/2} \frac{2}{\sqrt{\pi}} \Gamma \left(\frac{s+3}{2}, \frac{A}{T} \right), \quad (2.6)$$

where Γ denotes an incomplete Euler gamma function [1]. So, for instance, a different temperature dependence is in order for different collision models: the simplest is $\nu_{34}^{12} = \beta$ for Maxwellian molecules with $A=0$, but it would be of the type $(A+T) \exp(-A/T)/\sqrt{T}$ for hard spheres, collapsing to \sqrt{T} in the case of negligible activation energy. Options analogous to (2.5) could be made for the endothermic cross section σ_{12}^{34} , with similar but different results, since, even in absence of any activation threshold, this cross section vanishes unless g is large enough to allow transfer of an amount of energy ΔE from the impinging kinetic energies to the chemical links. For instance, with a Maxwellian-like cross section on its natural support, namely

$$\sigma_{12}^{34}(g, \psi) = \beta g^{-1} H \left[g^2 - \frac{2(m^1 + m^2)\Delta E}{m^1 m^2} \right] \gamma(\psi), \quad (2.7)$$

we would obtain the non-constant collision frequency

$$\nu_{34}^{12}(T) = \beta \exp\left(\frac{\Delta E}{T}\right) \frac{2}{\sqrt{\pi}} \Gamma\left(\frac{3}{2}, \frac{\Delta E}{T}\right). \quad (2.8)$$

As anticipated, equations (2.1) express balance in a proper phase space, ignoring effects like viscosity and thermal conductivity, but containing collision contributions, represented by the chemical source (2.2). The limiting case of a “frozen” gas is recovered when $\nu_{ij}^{hk} = 0$, yielding the standard inert Euler equations for the mixture. In the reactive case, searching for collision equilibria amounts merely to setting $Q = 0$, which immediately gives, due to (2.4), the law of mass action (1.3). The exact conservation equations following from (2.1) are easily obtained as

$$\begin{aligned} \frac{\partial}{\partial t}(n^i + n^j) + \frac{\partial}{\partial x}[(n^i + n^j)u] &= 0 \quad (i, j) = (1, 3), (1, 4), (2, 4) \\ \frac{\partial}{\partial t}(\rho u) + \frac{\partial}{\partial x}(\rho u^2 + nT) &= 0 \\ \frac{\partial}{\partial t}\left(\frac{1}{2}\rho u^2 + \frac{3}{2}nT + \sum_{i=1}^4 E^i n^i\right) + \frac{\partial}{\partial x}\left(\frac{1}{2}\rho u^3 + \frac{5}{2}nTu + \sum_{i=1}^4 E^i n^i u\right) &= 0, \end{aligned} \quad (2.9)$$

a set of five hyperbolic equations [6] for the six unknown fields involved. The zero-order closure of this set consists just in eliminating one of the unknowns by using collision equilibrium (1.3), and in this sense equation (2.9) may be regarded as reactive Euler equations associated to the model (2.1), which is of fluid-dynamic type, but yet includes collision terms. Equations (2.9) and (1.3) indeed constitute the closed set governing evolution in the limiting case of an “equilibrium” gas.

In view of the analysis developed in the next sections, here we recall the main facts characterizing both limiting situations. In the frozen limit of an inert gas, the sound speed for any equilibrium state has the well known expression

$$c_0^2 = \frac{5}{3} \frac{nT}{\rho}. \quad (2.10)$$

Shock structure is provided by the steady solution of the inert version of (2.1) joining two equilibrium states at $\pm\infty$, and once the 6 upstream parameters (n_-^i, u_-, T_-) are given, the corresponding downstream quantities are determined by the Rankine-Hugoniot conditions. The upstream Mach number $M_0 = u_-/c_{0-}$ is bound to be greater than unity (the wave front must be supersonic). In particular, for later reference,

$$u_+ = \frac{\rho_- u_-^2 + 5n_- T_-}{4\rho_- u_-}, \quad T_+ = \frac{3\rho_- u_-^2 - n_- T_-}{\rho_- u_-^2 + 5n_- T_-} \frac{\rho_- u_-^2}{n_-}. \quad (2.11)$$

As is well known, the only admissible solution is a weak solution, which is piecewise constant and equal to the pertinent upstream or downstream asymptotic state, with a jump (first order discontinuity) joining the two branches, at an abscissa which remains arbitrary and can be localized anywhere, because of the obvious Galilean invariance.

In the equilibrium limit of an infinitely fast reaction, the sound speed is given by [6, 19]

$$c = \alpha c_0, \quad \alpha^2 = \frac{\sum_{i=1}^4 \frac{1}{\chi^i} + \frac{2}{5} \left(\frac{\Delta E}{T}\right)^2}{\sum_{i=1}^4 \frac{1}{\chi^i} + \frac{2}{3} \left(\frac{\Delta E}{T}\right)^2} \quad (2.12)$$

with $3/5 < \alpha^2 < 1$, where there are only five unknown fields, with, for instance, temperature determined by concentrations as prescribed by the law of mass action (1.3). Discussion of the shock problem and of the relevant conservation equations and entropy condition is quite involved, and we refer to [15] for details (the results indeed apply at any level of description, including kinetic). Downstream parameters (n_+, u_+) are again uniquely determined by the upstream ones by reactive Rankine-Hugoniot conditions (omitted here), and the admissibility condition of the shock is that the upstream Mach number $M = u_-/c_-$ must be greater than one. In particular, we have $n_+ > n_-$, $T_+ > T_-$, $u_+ < u_-$, and, as regards the chemical composition,

$$\chi_+^i - \chi_-^i = \Lambda^i \Delta\chi, \quad \Delta\chi < 0. \quad (2.13)$$

Also in this case only a weak solution is possible, which is piecewise constant and equal to one of the asymptotic states with a jump joining them at arbitrary abscissa. Next, we shall fill the gap between such frozen and equilibrium situations by investigating the intermediate case of finite and non-vanishing ν_{ij}^{hk} , as described by (2.1), (2.2).

3. Dispersion relation

The set (2.1) may be rewritten in convective form, and expansion around a stationary homogeneous state at zero drift leads to the following linearized set for the small perturbations $(\tilde{n}^i, \tilde{u}, \tilde{T})$

$$\begin{aligned} \frac{\partial \tilde{n}^i}{\partial t} + \hat{n}^i \frac{\partial \tilde{u}}{\partial x} &= \Lambda^i q \quad i = 1, 2, 3, 4 \\ \frac{\partial \tilde{u}}{\partial t} + \frac{\hat{n}}{\hat{\rho}} \frac{\partial \tilde{T}}{\partial x} + \frac{\hat{T}}{\hat{\rho}} \frac{\partial \tilde{n}}{\partial x} &= 0 \\ \frac{\partial \tilde{T}}{\partial t} + \frac{2}{3} \hat{T} \frac{\partial \tilde{u}}{\partial x} &= \frac{2}{3} \frac{\Delta E}{\hat{n}} q, \end{aligned} \quad (3.1)$$

where a hat denotes the reference state and

$$q = \hat{\nu}_{12}^{34} \left(-\hat{n}^2 \tilde{n}^1 - \hat{n}^1 \tilde{n}^2 + \frac{\hat{n}^1 \hat{n}^2}{\hat{n}^3} \tilde{n}^3 + \frac{\hat{n}^1 \hat{n}^2}{\hat{n}^4} \tilde{n}^4 - \frac{\Delta E}{\hat{T}} \frac{\hat{n}^1 \hat{n}^2}{\hat{T}} \tilde{T} \right). \quad (3.2)$$

The usual ansatz $\tilde{\phi}(x, t) = \bar{\phi} \exp(\lambda t + ikx)$, with ϕ standing for any of the symbols n^i, u, T yields, after removing all hats, a homogeneous algebraic system for $\bar{n}^i, \bar{u}, \bar{T}$. At this point, the reactive dispersion relation is obtained by setting the determinant of the relevant matrix

$$\begin{pmatrix} \lambda + \nu_{12}^{34} n^2 & \nu_{12}^{34} n^1 & -\frac{\nu_{12}^{34} n^1 n^2}{n^3} & -\frac{\nu_{12}^{34} n^1 n^2}{n^4} & ikn^1 & \frac{\nu_{12}^{34} n^1 n^2}{T} \frac{\Delta E}{T} \\ \lambda & 0 & \lambda & 0 & ik(n^1 + n^3) & 0 \\ \lambda & 0 & 0 & \lambda & ik(n^1 + n^4) & 0 \\ 0 & \lambda & 0 & \lambda & ik(n^2 + n^4) & 0 \\ 0 & 0 & 0 & 0 & \lambda + \frac{k^2}{\lambda} \frac{nT}{\rho} & ik \frac{n}{\rho} \\ \lambda & 0 & 0 & 0 & ik \left(n^1 - \frac{T}{\Delta E} n \right) & -\frac{3}{2} \lambda \frac{n}{\Delta E} \end{pmatrix} \quad (3.3)$$

equal to zero, which yields a sixth degree polynomial with respect to λ . Along with the triple root $\lambda = 0$, there are three non-trivial k -dependent roots, which are solutions of the cubic equation

$$\tau \lambda^3 + \lambda^2 + \tau k^2 c_0^2 \lambda + k^2 c^2 = 0 \quad \text{or} \quad \lambda(\lambda^2 + k^2 c_0^2) + \frac{1}{\tau} (\lambda^2 + k^2 c^2) = 0, \quad (3.4)$$

where c_0 and c are provided by (2.10) and (2.12) and τ is the characteristic time defined by

$$\frac{1}{\tau} = \frac{\nu_{12}^{34}(T)n^1n^2}{n} \left[\sum_{i=1}^4 \frac{1}{\chi^i} + \frac{2}{3} \left(\frac{\Delta E}{T} \right)^2 \right], \quad (3.5)$$

which represents, as it is easily seen, the relaxation time for small space-homogeneous ($k=0$) perturbations. The limit $\tau \rightarrow 0$ (infinitely fast reaction) recovers the equilibrium scenario, with $\lambda = \pm ikc$; namely, plane-wave initial perturbations propagate forward and backward at the reactive sound speed c . The opposite limit $\tau \rightarrow +\infty$ (absence of reaction) leads back to the frozen scenario, with $\lambda = \pm ikc_0$; namely, plane-wave initial perturbations propagate as before, but at the inert sound speed c_0 . In all intermediate cases $\tau \in (0, +\infty)$, there are instead three fundamental modes, and the eigenvalues may be complex conjugate pairs, $\lambda = a + ib$, with a quantifying possible damping or explosion in time and b providing the phase velocity of the traveling wave via the ratio b/k . One of the roots of (3.4) is necessarily, by its own sign structure, real and negative, so that one of the modes describes relaxation without propagation of the considered perturbations. It is possible indeed to prove that the other two roots are a complex conjugate pair. In fact, the condition for that is

$$\frac{1}{27}z^2 + \left(\frac{1}{4}\alpha^4 - \frac{1}{6}\alpha^2 - \frac{1}{108} \right) z + \frac{1}{27}\alpha^2 > 0, \quad z = \tau^2 k^2 c_0^2, \quad (3.6)$$

with $\alpha = c/c_0$ defined in (2.12), which is always true because the left hand side is a positive definite quadratic form for $\alpha^2 = 3/5$ and increases for increasing α . In addition, it is not difficult to see that the real part of the pair is negative, implying damping as expected. In conclusion, the fundamental modes are given by

$$\exp(\lambda_1 t) \exp(ikx), \quad \exp(at) \exp[i(kx + bt)], \quad \exp(at) \exp[i(kx - bt)], \quad (3.7)$$

where

$$\begin{aligned} \lambda_1 &= \frac{1}{\tau} \left(r_+ + r_- - \frac{1}{3} \right) < 0, \\ a &= -\frac{1}{\tau} \left(\frac{r_+}{2} + \frac{r_-}{2} + \frac{1}{3} \right) < 0, \quad b = \frac{1}{\tau} \frac{\sqrt{3}}{2} |r_+ - r_-| > 0, \end{aligned} \quad (3.8)$$

with

$$r_{\pm} = \left\{ \left(\frac{1}{6} - \frac{1}{2}\alpha^2 \right) z - \frac{1}{27} \pm \left[\frac{1}{27}z^3 + \left(\frac{1}{4}\alpha^4 - \frac{1}{6}\alpha^2 - \frac{1}{108} \right) z^2 + \frac{1}{27}\alpha^2 z \right]^{1/2} \right\}^{1/3}. \quad (3.9)$$

Dependence on the wave number k and on the strength of the chemical source is accounted for by the characteristic time τ , which is inversely proportional to the chemical reaction rate, and by the dimensionless parameters z and α , which involve both reactive and inert sound speeds. It might be interesting to estimate the trend of the crucial parameters λ_1 , a , and b for very fast or very slow reactions. It is only matter of some algebra to show that

$$\lambda_1 = -\frac{1}{\tau} + O(\tau), \quad a = -\frac{k^2}{2}(c_0^2 - c^2)\tau + O(\tau^2), \quad \frac{b}{k} = c + O(\tau^2), \quad (3.10)$$

for $\tau \rightarrow 0$, and

$$\lambda_1 = -\frac{\alpha^2}{\tau} + O\left(\frac{1}{\tau^2}\right), \quad a = -\frac{1-\alpha^2}{2\tau} + O\left(\frac{1}{\tau^2}\right), \quad \frac{b}{k} = c_0 + O\left(\frac{1}{\tau^2}\right), \quad (3.11)$$

for $\tau \rightarrow +\infty$, which reproduces the limiting equilibrium and frozen situations and provides first order corrections. Similar analysis holds with respect to the wave number k , and results in

$$\lambda_1 = -\frac{1}{\tau} + O(k^2), \quad a = -\frac{\tau}{2}(c_0^2 - c^2)k^2 + O(k^3), \quad \frac{b}{k} = c + O(k^2), \quad (3.12)$$

for $k \rightarrow 0$, and

$$\lambda_1 = -\frac{\alpha^2}{\tau} + O\left(\frac{1}{k}\right), \quad a = -\frac{1-\alpha^2}{2\tau} + O\left(\frac{1}{k}\right), \quad \frac{b}{k} = c_0 + O\left(\frac{1}{k^2}\right), \quad (3.13)$$

for $k \rightarrow +\infty$.

4. Shock wave structure

The steady shock problem may be formulated in the usual way [22], and one looks for solutions (n^i, u, T) to the stationary version of (2.1) with given asymptotic conditions $(n_{\pm}^i, u_{\pm}, T_{\pm})$ for $x \rightarrow \pm\infty$. Asymptotic states must be in chemical equilibrium, thus the law of mass action must hold for both boundary data

$$\frac{\Delta E}{T_{\pm}} = \sum_{i=1}^4 \Lambda^i \log \frac{\chi_{\pm}^i}{(m^i)^{3/2}}, \quad (4.1)$$

leaving only five free parameters on each side. As recalled above, parameters at $+\infty$ are uniquely determined by those at $-\infty$ by the Rankine-Hugoniot conditions established in [15], and the upstream velocity u_- must be greater than the pertinent sound speed c_- ($M > 1$, supersonic wave), a constraint that also implies (2.13). From (2.9), five first-integrals must be in order, namely

$$\begin{aligned} (n^i + n^j)u &= \text{const.} & (i, j) &= (1, 3), (1, 4), (2, 4) \\ \rho u^2 + nT &= \text{const.} \\ \frac{1}{2}\rho u^3 + \frac{5}{2}nTu + \sum_{i=1}^4 E^i n^i u &= \text{const.}, \end{aligned} \quad (4.2)$$

where the constants are determined by the assigned upstream conditions, and where u is not allowed to change sign so that we may conventionally assume it to be positive. Equations (4.2) permit in principle to express all unknown fields in terms of a single dependent variable, leaving only one ordinary differential equation to be actually solved; for instance the first equation in (2.1). In this respect, the present model is certainly the simplest non-trivial tool of investigation for the considered bimolecular reaction, because of its drastic reduction to only one degree of freedom (a one-dimensional dynamical system). It will then be worth comparing its results to the outputs from other less idealized but more complicated approaches.

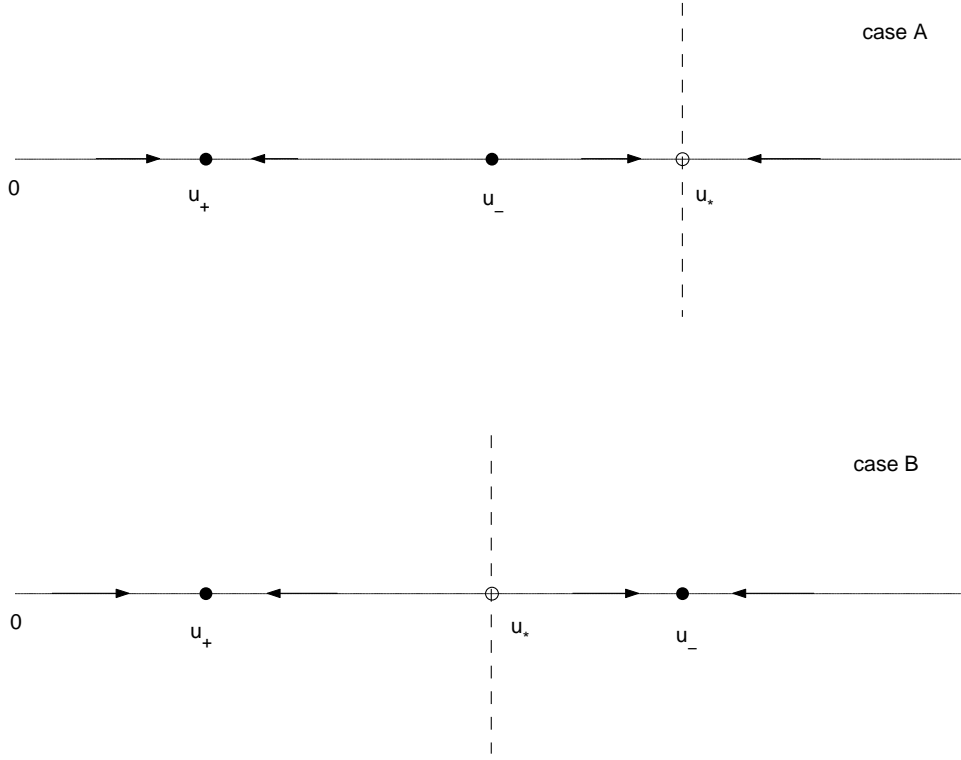


FIG. 4.1. One-dimensional phase diagram for the variable u versus x in equation (4.4), with the different locations of the equilibrium points u_- , u_+ and of the singular point u_* in the two cases A and B; arrows indicate vector field and trend of solution for x increasing from $-\infty$ to $+\infty$.

Specifically, all variables may be eliminated in terms of $u > 0$ as

$$\begin{aligned}
 n &= \frac{n_- u_-}{u} & \rho &= \frac{\rho_- u_-}{u} \\
 T &= \frac{\rho_- u_-^2 + n_- T_-}{n_- u_-} u - \frac{\rho_-}{n_-} u^2 & n^i &= \frac{n_-^i u_-}{u} - \Lambda^i N \\
 N &= \frac{1}{\Delta E} \left[2\rho_- u_- u - \frac{5}{2}(\rho_- u_-^2 + n_- T_-) + \left(\frac{1}{2}\rho_- u_-^3 + \frac{5}{2}n_- T_- u_- \right) \frac{1}{u} \right]
 \end{aligned} \tag{4.3}$$

where the admissible range of u itself must be tested versus positivity of the fields n^i and T , and the whole problem reduces to

$$\frac{d}{dx} F(u) = G(u) \quad \lim_{x \rightarrow \pm\infty} u(x) = u_{\pm}, \tag{4.4}$$

where $F(u)$ and $G(u)$ are nothing but the quantities $n^1 u$ and Q once they have been made explicit through (4.3). In particular

$$F(u) = n_-^1 u_- - \frac{1}{\Delta E} \left[2\rho_- u_- u^2 - \frac{5}{2}(\rho_- u_-^2 + n_- T_-)u + \frac{1}{2}\rho_- u_-^3 + \frac{5}{2}n_- T_- u_- \right]. \tag{4.5}$$

Even though (4.4) can not be solved analytically, it lends itself to a direct application of the qualitative theory of dynamical systems, which allows us to extract all necessary

information on the basis of the relevant vector field only, specifically by studying zeroes and possible singular points of the known functions $G(u)$ and $F'(u) = dF/du$. From [15] we can rely on the fact that the smooth function G has exactly two simple zeroes at $u = u_{\pm}$ corresponding to the two equilibria compatible with the upstream conditions and that G must be negative on the interval $u \in (u_+, u_-)$, due to the constraint (2.13). In addition, F' follows trivially from (4.5) and is linear in u , with

$$F'(u) \geq 0 \quad \iff \quad u \leq u_*, \quad u_* = \frac{5}{8} \frac{\rho_- u_-^2 + n_- T_-}{\rho_- u_-}. \quad (4.6)$$

The zero at $u = u_*$ makes the equation singular and prevents existence of a global solution. In any case, we are able to determine the phase diagram on its one-dimensional phase space simply from the knowledge of the three critical points above, and the collocation of u_* with respect to u_+ and u_- , with $u_+ < u_-$, being crucial, as shown by figure 4.1. Note that

$$u_* \geq u_- \quad \iff \quad u_-^2 \leq \frac{5n_- T_-}{3\rho_-} = c_{0-}^2 \quad \iff \quad M_0 \leq 1, \quad (4.7)$$

where c_{0-} is the sound speed that the considered mixture would have, if it were chemically inert, in correspondence to the given upstream conditions, and M_0 is the associated (inert) Mach number. In other words, u_* is above u_- as long as $M < 1/\alpha_-$ with α_- defined by (2.12) (case A), but then it crosses that threshold and enters the strip (u_+, u_-) as soon as M exceeds $1/\alpha_-$, in which case (case B) even M_0 exceeds 1, and a shock structure also appears for the fictitious inert mixture.

In all cases the sign of the vector field determines the trend of phase trajectories, as shown by figure 4.1.

It is easy to check that if u_* were allowed to descend below the threshold u_+ , neither the boundary condition at $-\infty$ nor the one at $+\infty$ could be fulfilled, excluding any chance to satisfy the shock problem.

One can easily realize that there exists only one smooth solution in case A, whose classical profile monotonically joins the asymptotic limits and may be shifted freely, so that it can always be adapted to the convention $u(0) = (u_+ + u_-)/2$. Its existence is then restricted to a quite small range of input parameters, namely

$$c_- < u_- < c_{0-} \quad \iff \quad M_0 < 1 < M \quad \iff \quad 1 < M < 1/\alpha_-, \quad (4.8)$$

where α_- is typically quite close to unity. No smooth solutions are possible instead in case B.

Like for the Euler equations recalled in section 2, the question arises whether weak solutions with a step discontinuity at some point x (that can be shifted as usual to the origin) may exist. One has to look for a piecewise smooth solution in the separate intervals $(-\infty, 0)$ and $(0, +\infty)$, satisfying boundary conditions in (4.4), and whose limits for $x \rightarrow 0^-$ and $x \rightarrow 0^+$, say u_m and u_p , fulfil the constraint following from (4.4) itself, namely $F(u_p) = F(u_m)$. On using (4.5) and bearing in mind (4.6) one obtains

$$\frac{u_p + u_m}{2} = \frac{5}{8} \frac{\rho_- u_-^2 + n_- T_-}{\rho_- u_-} = u_*, \quad (4.9)$$

meaning that the previously discussed singular value $u = u_*$ exactly represents the midpoint of any admissible jump. A careful analysis shows that this is impossible in

case A, and that in case B the only branch tending to the right limit for $x \rightarrow -\infty$ is the constant solution $u = u_-$, which implies that u_m is equal to u_- and yields

$$u_p = 2u_* - u_- = \frac{\rho_- u_-^2 + 5n_- T_-}{4\rho_- u_-} = u_{0+}, \tag{4.10}$$

with u_{0+} standing for the downstream velocity of the inert mixture (frozen situation, see (2.11)). The jump then coincides with the step discontinuity that would occur if the reaction were switched off, and that would lead to a downstream state in chemical non-equilibrium. It is important to realize that u_{0+} , which is meaningful only for $M > 1/\alpha_-$ ($M_0 > 1$), never coincides with the actual downstream velocity u_+ . In fact, assuming the opposite, the two downstream states would coincide completely, which is an evident contradiction since the actual one must be characterized by $\Delta\chi < 0$ [15] whereas the inert one necessarily corresponds to $\Delta\chi = 0$. Since u_{0+} is initially equal to $u_- > u_+$ at $M = 1/\alpha_-$, it remains greater than u_+ for all larger M . At this point, the weak solution is completed by a smooth branch on the positive real axis starting out from u_{0+} and asymptotically approaching u_+ , and it is easily seen that no undershooting is possible for u . Putting these pieces together, we obtain actually the only possible weak solution, satisfying the variational form

$$\int_{-\infty}^{+\infty} \left[F(u) \frac{d\varphi}{dx} + G(u)\varphi(x) \right] dx = 0 \tag{4.11}$$

for any suitably smooth test function φ (e.g. $\varphi \in C_0^1(\mathbb{R})$), relevant to the range

$$u_- > c_{0-} \iff M_0 > 1 \iff M > 1/\alpha_-, \tag{4.12}$$

complementary to (4.8), in which we have instead a smooth solution. The range for the smooth solution is quite small ($1/\alpha$ can never exceed $\sqrt{5/3} \approx 1.291$, whatever the upstream composition, but is often significantly lower), and the bifurcation value is just $M_0 = 1$, in agreement with the fact that a shock structure does not exist in the absence of reaction when $M_0 \leq 1$. At the bifurcation, the non-constant branch starts out at $u = u_* = u_-$ for $x = 0$, with zero jump, but with infinite initial slope.

We can quantify the effects of variation of the physical parameters on the shock structure as follows. For M increasing from unity upwards, the smooth monotonic velocity profile sharpens, and at the same time the separation of the asymptotes increases, until bifurcation occurs at $M = 1/\alpha_-$; then the wave front steepens and develops a jump discontinuity that keeps on enlarging for increasing M . As in similar thermodynamic problems [23], though the equations are of hydrodynamic type, there is a small region in parameter space in which non-equilibrium processes have a dissipative effect and allow a smooth solution, whereas in most of the space the solution necessarily presents a discontinuity, corresponding to the frozen limit, followed by a smooth tail leading to equilibrium conditions. In addition, for the present reactive model, it is very easy to study the effects of the strength of the chemical source on the solution when all other parameters are fixed. In fact, the dependence on the microscopic collision frequency ν_{ij}^{hk} is simply linear in the reaction rate Q , and then in the right hand side of (4.4), so that it affects the solution only as a scaling factor for the variable x . Therefore, if ν_{ij}^{hk} becomes larger and larger, the profile steepens more and more, approaching as expected the step profile which is in order in the equilibrium limit (see section 2). The other limit, when ν_{ij}^{hk} becomes smaller and smaller, is more delicate, especially in the smooth case $M < 1/\alpha_-$, and deserves future investigation. It is clear however how the profile becomes instead flatter and flatter, and how the weak solution now approaches the frozen limit.

5. Numerical results and final comments

For illustrative purposes, in this section we explicitly show the shock profiles resulting from the numerical integration of (4.4) for various choices of parameters (chemical reaction, collision model, upstream conditions, and Mach number). All results are dimensionless as stipulated at the beginning, so that in particular ΔE is understood to be unity. Conversion to actual scales is then different for different reactions. Smooth solutions are normalized in such a way that $u(0) = (u_- + u_+)/2$, and are obtained by integrating forward and backward from such initial conditions. For weak solutions instead the jump is localized at $x=0$, and the smooth tail is obtained by integrating forward from the initial condition $u(0) = u_{0+}$. All numerical integrations were performed by using standard Runge-Kutta methods, on uniform or adaptive grids.

Collision models adopted in the results presented here include exothermic Maxwell molecules

$$\nu_{34}^{12} = 1, \quad (5.1)$$

exothermic Maxwell molecules with activation energy $A > 0$

$$\nu_{34}^{12}(T) = \frac{2}{\sqrt{\pi}} \Gamma\left(\frac{3}{2}, \frac{A}{T}\right), \quad (5.2)$$

and exothermic hard spheres

$$\nu_{34}^{12}(T) = \frac{2}{\sqrt{\pi}} \left(\frac{2(m^3 + m^4)T}{m^3 m^4} \right)^{1/2}. \quad (5.3)$$

Multiplicative factors applied to these parameters induce merely a different x -scale, as discussed in the previous section.

As reference reaction we take $H_2O + H \rightleftharpoons OH + H_2$, corresponding to (dimensionless) masses

$$m^1 = 1.8, \quad m^2 = 0.1, \quad m^3 = 1.7, \quad m^4 = 0.2.$$

As reference upstream conditions we take the situation defined by $n_- = 1.85$ and by concentration fractions

$$\chi_-^1 = 0.4324, \quad \chi_-^2 = 0.4865, \quad \chi_-^3 = 0.0270, \quad \chi_-^4 = 0.0541, \quad (5.4)$$

from which $T_- = 0.1688$. There follows

$$c_{0-} = 0.5642, \quad c_- = 0.5316, \quad \alpha_- = 0.9421. \quad (5.5)$$

The bifurcation value for the Mach number is then $M = 1/\alpha_- = 1.0614$. This test case will be labeled below as Problem A.

Once u_- (or, equivalently, M) is also given, all downstream parameters are uniquely determined by the previously discussed Rankine-Hugoniot conditions. We plot the quantities u_- , u_+ , u_{0+} , u_* , and M_0 versus $M > 1$ in figure 5.1, where one may observe the splitting of u_+ and u_- at $M=1$, and of u_{0+} and u_- at $M_0=1$ ($M=1/\alpha_-$). Of course, u_- and M_0 are linear in M , and u_{0+} is meaningless for $M < 1/\alpha_-$; in addition, as discussed, u_{0+} is greater than u_+ for any M .

We then show the shock profiles starting from the collision model of exothermic Maxwell molecules (5.1). We select six different values of the Mach number above and below the bifurcation value by six different choices of $\Delta\chi$:

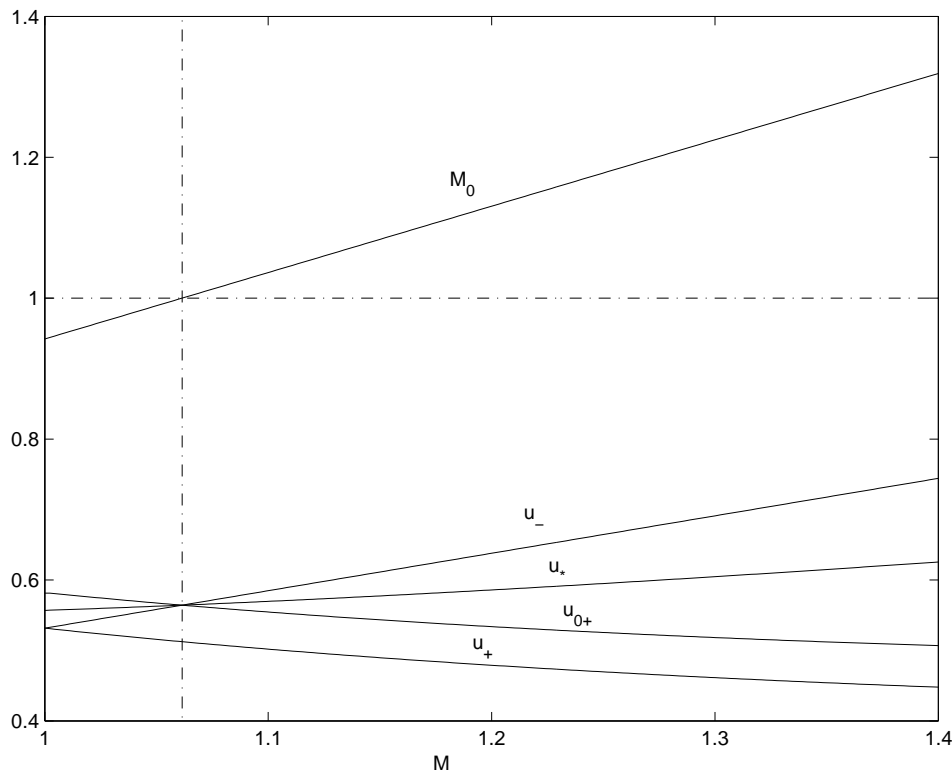


FIG. 5.1. Typical parameters determining the shock profile (u_- , u_+ , u_{0+} , u_* , and M_0) versus the Mach number $M > 1$ for the reaction and upstream conditions of the test case (Problem A).

- a) $\Delta\chi = -0.1 \Leftrightarrow M = 2.2639$;
 $u_- = 1.2035$ $u_+ = 0.4265$ $u_* = 0.8514$ $u_{0+} = 0.4993$
- b) $\Delta\chi = -0.05 \Leftrightarrow M = 1.6392$;
 $u_- = 0.8714$ $u_+ = 0.4281$ $u_* = 0.6816$ $u_{0+} = 0.4919$
- c) $\Delta\chi = -0.01 \Leftrightarrow M = 1.1298$;
 $u_- = 0.6006$ $u_+ = 0.4944$ $u_* = 0.5742$ $u_{0+} = 0.5477$
- d) $\Delta\chi = -0.005 \Leftrightarrow M = 1.0647$ ($M_0 = 1.0031$);
 $u_- = 0.5660$ $u_+ = 0.5115$ $u_* = 0.5647$ $u_{0+} = 0.5634$
- e) $\Delta\chi = -0.004 \Leftrightarrow M = 1.0517$ ($M_0 = 0.9909$);
 $u_- = 0.5591$ $u_+ = 0.5153$ ($u_* = 0.5630$)
- f) $\Delta\chi = -0.001 \Leftrightarrow M = 1.0129$ ($M_0 = 0.9543$);
 $u_- = 0.5385$ $u_+ = 0.5273$ ($u_* = 0.5583$).

In figure 5.2 the velocity u is plotted versus x for all options a)–f), with smooth solution in e) and f) (below the threshold), and discontinuous solution otherwise (above the threshold). The crucial parameters u_- , u_+ , u_* are marked for convenience, and cases d) and e) are just across the bifurcation. As a general fact, the almost symmetric smooth trend between quite close asymptotes, in order for small M , gets strained and sharpened at the upstream front when M increases and approaches bifurcation, and at the same time asymptotes separate more and more. Beyond this threshold the singularity develops, though the shape seems unchanged across it

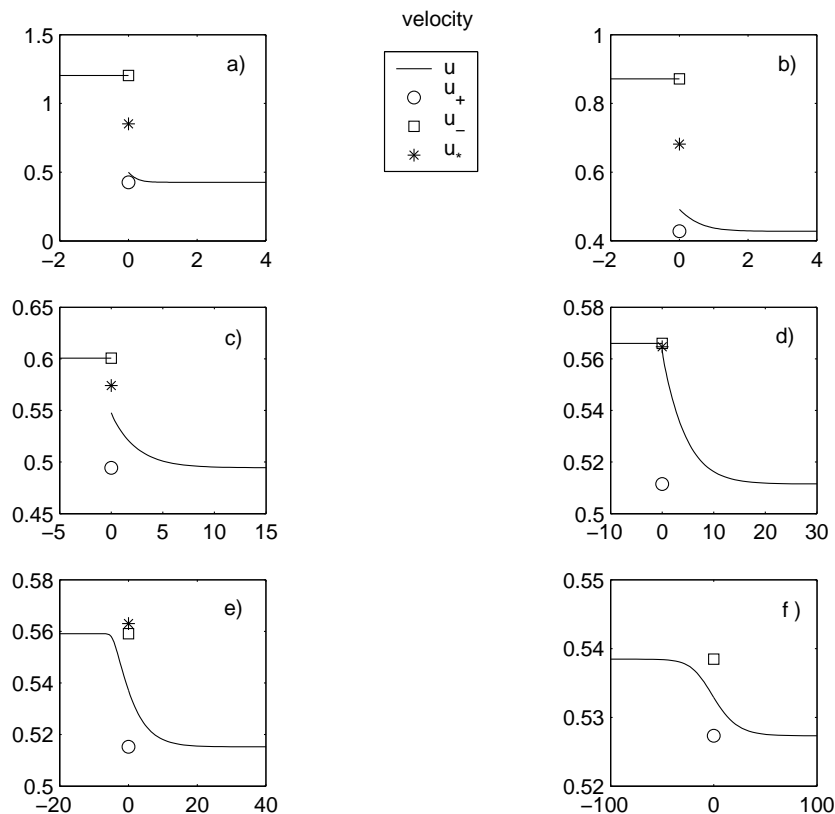


FIG. 5.2. Velocity versus x for the Mach numbers relevant to the six options a)–f) (Problem A) when collisions are modeled according to exothermic Maxwell molecules.

(notice the different collocation of the reference abscissa $x=0$ in the two cases). If M continues to increase, the discontinuity becomes larger and larger, covering a higher and higher fraction of the overall jump from u_- to u_+ , which in turn also increases. The smooth tail leading from u_{0+} to u_+ , describing the slow chemical relaxation [23], becomes very flat for intermediate or high values of M . The other physical quantities characterizing the mixture follow directly from the knowledge of velocity by simply using (4.3). Number densities are reported in figure 5.3, with the same layout of figure 5.2, but restricted for brevity to the cases a)–d). One may also observe, along with the expected increase of the jump discontinuity for increasing M , the appearance of overshooting in the relaxation tail for some of the densities (the two reactants, for which the inert jump is larger than the reactive one) at large Mach numbers. Temperature is shown for the same four cases as before in figure 5.4, and exhibits in a sense a similar trend; actually, overshooting occurs when the Mach number increases, and it starts appearing at lower values than for densities.

Figures 5.5 and 5.6 briefly illustrate the effects of a different collision model on the same reaction with the same upstream conditions, by comparing the velocity profiles to the corresponding ones of the reference case, as given by figure 5.2. In general, the main features in the trends remain unchanged, and one can mainly observe the different effectiveness of collisions in driving the process. Figure 5.5 differs from

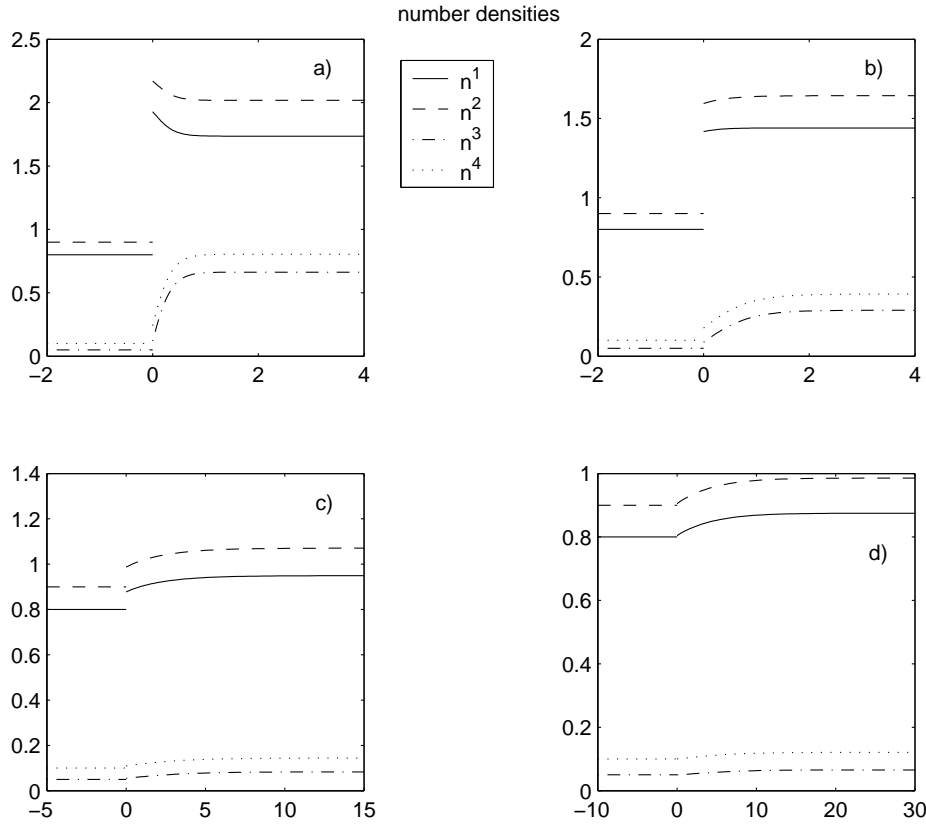


FIG. 5.3. Number densities versus x for the Mach numbers relevant to the four options a), b), c) d) (Problem A) when collisions are modeled according to exothermic Maxwell molecules.

the reference case because of the occurrence of a positive activation energy A , as prescribed by (5.2). As expected, the higher the activation, the fewer the chemical reactions, so that the effect is a slower approach to the asymptotes and an enlarged shock thickness. Another expected result evident from the plots is the nonlinear dependence on the threshold A itself. Indeed, for A ranging from 0 to about 0.15 the difference with respect to the case $A=0$ is hardly visible in the plots. Finally, figure 5.6 is relevant to the exothermic hard sphere model, and the effectiveness of the reaction is measured now by the value of the right hand side of (5.3) in comparison to unity. It can be verified that for the present reaction and upstream condition such a ratio is greater than one, which explains the observed decrease in the shock thickness, but of course this effect could be reversed for different reactions or input parameters (see for instance [19]).

Next, sticking to the exothermic Maxwell model (5.1) of the test case, let us consider a different upstream condition, still with $n_- = 1.85$, but with more balanced concentration fractions

$$\chi_-^1 = 0.25, \quad \chi_-^2 = 0.35, \quad \chi_-^3 = 0.25, \quad \chi_-^4 = 0.15, \quad (5.6)$$

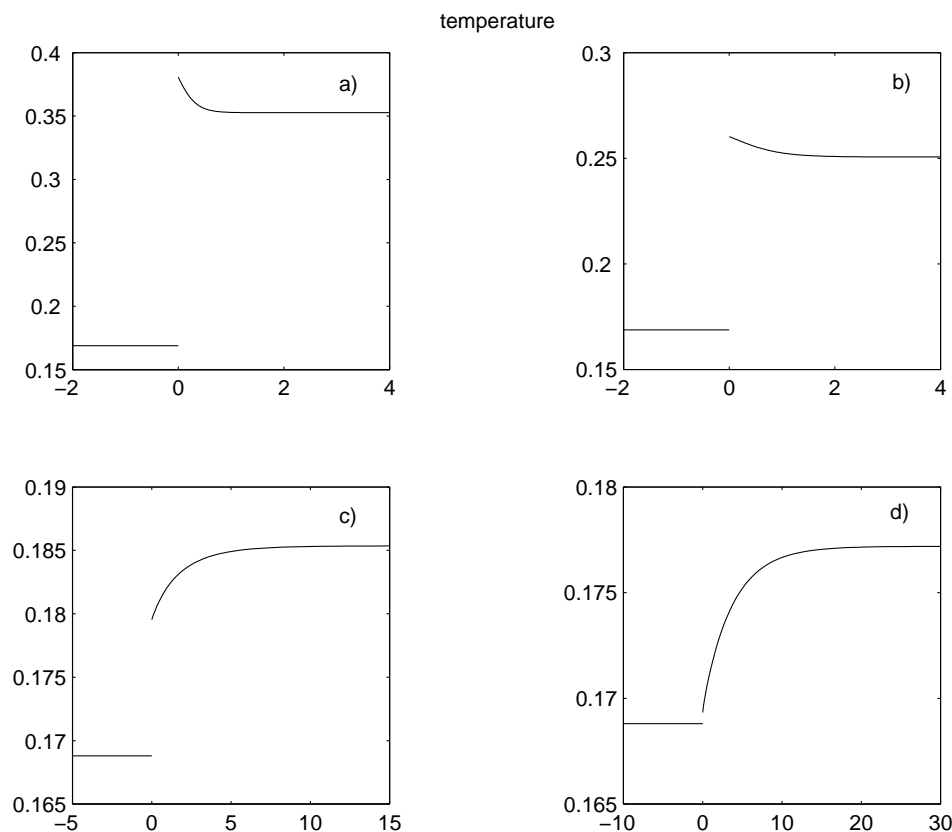


FIG. 5.4. Temperature versus x for the Mach numbers relevant to the four options a), b), c) d) (Problem A) when collisions are modeled according to exothermic Maxwell molecules.

from which $T_- = 0.5552$. There follows

$$c_{0-} = 0.9921, \quad c_- = 0.9701, \quad \alpha_- = 0.9778. \quad (5.7)$$

The bifurcation value for the Mach number is now $M = 1/\alpha_- = 1.0227$. We shall label this problem as Problem B. Since, apart from the different values of downstream parameters and singular points, the behaviors are essentially the same as for the test case, we report only, in figure 5.7, the number densities for the following four values of the Mach number corresponding to four different choices of $\Delta\chi$:

- a) $\Delta\chi = -0.05 \Leftrightarrow M = 1.9083$;
 $u_- = 1.8512 \quad u_+ = 0.8354 \quad u_* = 1.3564 \quad u_{0+} = 0.8616$
- b) $\Delta\chi = -0.01 \Leftrightarrow M = 1.1203$;
 $u_- = 1.0868 \quad u_+ = 0.9192 \quad u_* = 1.0189 \quad u_{0+} = 0.9510$
- c) $\Delta\chi = -0.004 \Leftrightarrow M = 1.0451$;
 $u_- = 1.0139 \quad u_+ = 0.9489 \quad u_* = 0.9977 \quad u_{0+} = 0.9816$
- d) $\Delta\chi = -0.003 \Leftrightarrow M = 1.0335 \quad (M_0 = 1.0105)$;
 $u_- = 1.0026 \quad u_+ = 0.9541 \quad u_* = 0.9948 \quad u_{0+} = 0.9870$.

The density profiles again show overshooting for reactants when the Mach number is large enough.

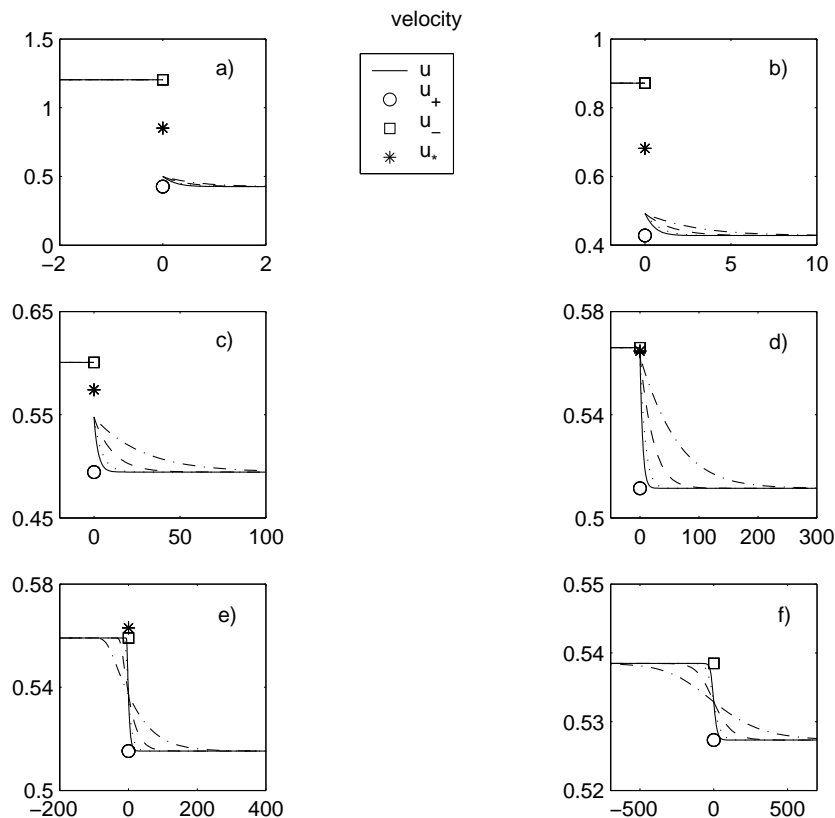


FIG. 5.5. Comparison of velocities obtained for the options a)–f) (Problem A) by using the collision model of exothermic Maxwell molecules with different activation threshold A : $A=0$ (solid line), $A=0.2$ (dotted line), $A=0.4$ (dashed line), and $A=0.6$ (dashed-dotted line).

Finally, in order to give an account of the several cases that have been run, we switch to the reaction $NO + CO_2 \rightleftharpoons NO_2 + CO$, corresponding to dimensionless masses

$$m^1 = 3, \quad m^2 = 4.4, \quad m^3 = 4.6, \quad m^4 = 2.8.$$

For the same collision model of the reference case (exothermic Maxwell molecules without activation barrier) and with upstream molar fractions given by (5.6), we plot in figure 5.8 number densities for the following four options of Mach numbers

- a) $\Delta\chi = -0.0200 \Leftrightarrow M = 1.7336$;
 $u_- = 1.2591 \quad u_+ = 0.6280 \quad u_* = 0.9456 \quad u_{0+} = 0.6321$
- b) $\Delta\chi = -0.0100 \Leftrightarrow M = 1.2856$;
 $u_- = 0.9338 \quad u_+ = 0.6567 \quad u_* = 0.7976 \quad u_{0+} = 0.6613$
- c) $\Delta\chi = -0.0010 \Leftrightarrow M = 1.0227$;
 $u_- = 0.7428 \quad u_+ = 0.7183 \quad u_* = 0.7332 \quad u_{0+} = 0.7236$
- d) $\Delta\chi = -0.0005 \Leftrightarrow M = 1.0112$ ($M_0 = 1.0063$);
 $u_- = 0.7345 \quad u_+ = 0.7223 \quad u_* = 0.7310 \quad u_{0+} = 0.7276$.

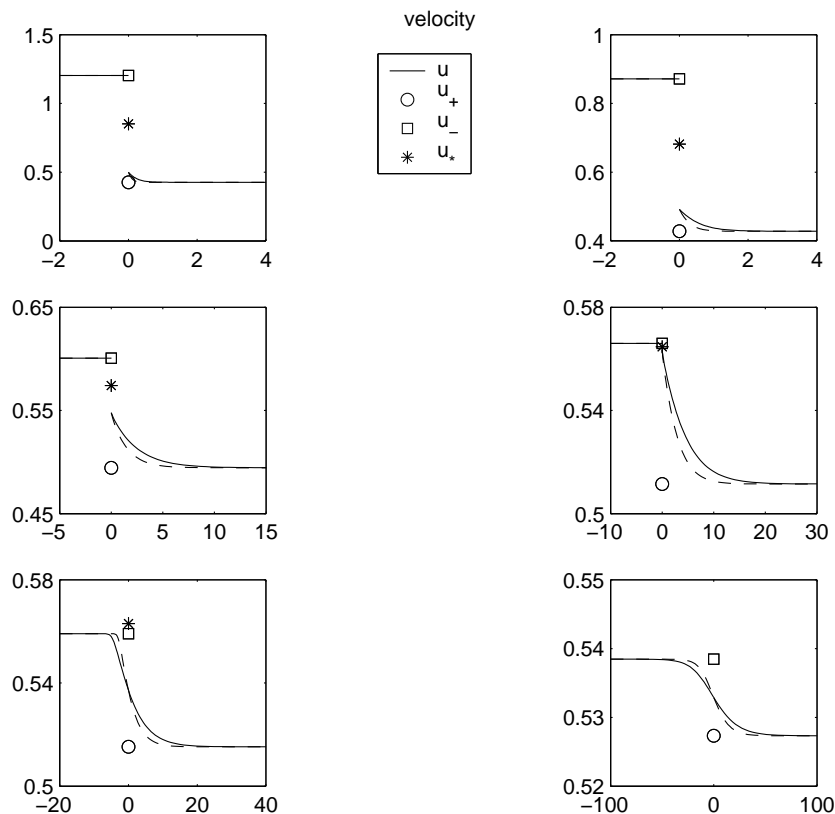


FIG. 5.6. Comparison of velocities obtained for the options a)–f) (Problem A) by using two different collision models: exothermic Maxwell molecules (solid line) and exothermic hard spheres (dashed line).

Now we have $T_- = 1.2338$ and bifurcation at $M = 1.0049$. This problem is labeled as Problem C. Again, overshooting of number densities (limited as usual to reactants) is triggered sooner or later when the Mach number keeps on increasing. Indeed, occurrence of such overshooting has been observed in all considered cases, only with a threshold that depends on the specific reaction, and on the boundary data within the same reaction. As regards temperature, which is not shown here for brevity, a similar trend seems to be in order, and the main difference with respect to the test case is that the threshold Mach for temperature is here higher than for densities.

Acknowledgement. This work was performed in the frame of the activities sponsored by MIUR (Project “Nonconservative binary interactions in various types of kinetic models”), by INdAM, by GNFM, and by the University of Parma (Italy).

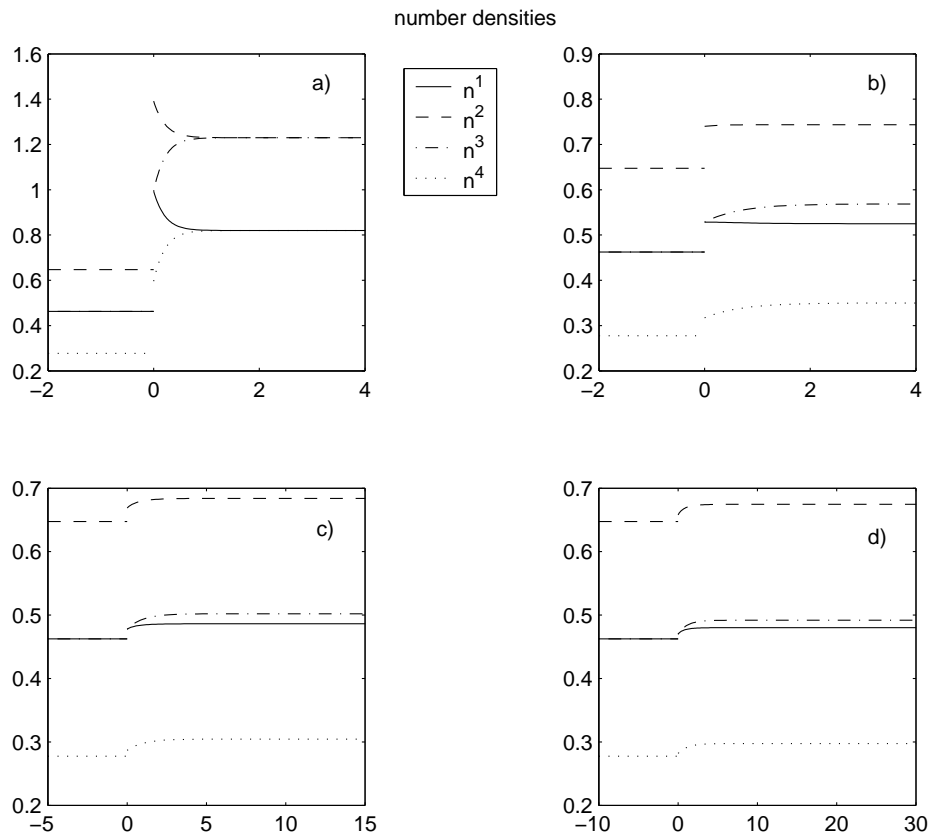


FIG. 5.7. Number densities versus x for the Mach numbers relevant to the four options a), b), c) d) (Problem B).

REFERENCES

- [1] M. Abramowitz and I.A. Stegun (Eds), *Handbook of Mathematical Functions*, Dover, New York, 1972.
- [2] A. Aimi, M. Diligenti, M. Groppi and C. Guardasoni, *On the numerical solution of a BGK-type model for chemical reactions*, *Europ. J. Mech./B Fluids*, 26, 455–472, 2007.
- [3] M. Bisi, M. Groppi and G. Spiga, *A kinetic model for bimolecular chemical reactions*, in *Kinetic Methods for Nonconservative and Reacting Systems*, G. Toscani. Quaderni di Matematica (ed.), Dipartimento di Matematica, Seconda Università di Napoli, Caserta. Aracne Editrice S.r.l., Roma, 16, 1–145, 2005.
- [4] C. Cercignani, *The Boltzmann Equation and its Applications*, Springer, New York, 1988.
- [5] J.F. Clarke and M. McChesney, *The Dynamics of Real Gases*, Butterworths, London, 1964.
- [6] F. Conforto, M. Groppi, R. Monaco and G. Spiga, *Steady detonation problem for slow and fast chemical reactions*, in *Modelling and Numerics of Kinetic Dissipative Systems*, L. Pareschi, G. Russo and G. Toscani (eds), Nova Science, New York, 105–117, 2006.
- [7] F. Conforto, R. Monaco, F. Schürer and I. Ziegler, *Steady detonation waves via the Boltzmann equation for a reacting mixture*, *J. Phys. A*, 36, 5381–5398, 2003.
- [8] L. Desvillettes, R. Monaco and F. Salvarani, *A kinetic model allowing to obtain the energy law of polytropic gases in the presence of chemical reactions*, *Europ. J. Mech./B Fluids*, 24, 219–236, 2005.
- [9] F. Filbet and G. Russo, *High order numerical methods for the space non-homogeneous Boltzmann equation*, *J. Comp. Phys.*, 186, 457–480, 2003.

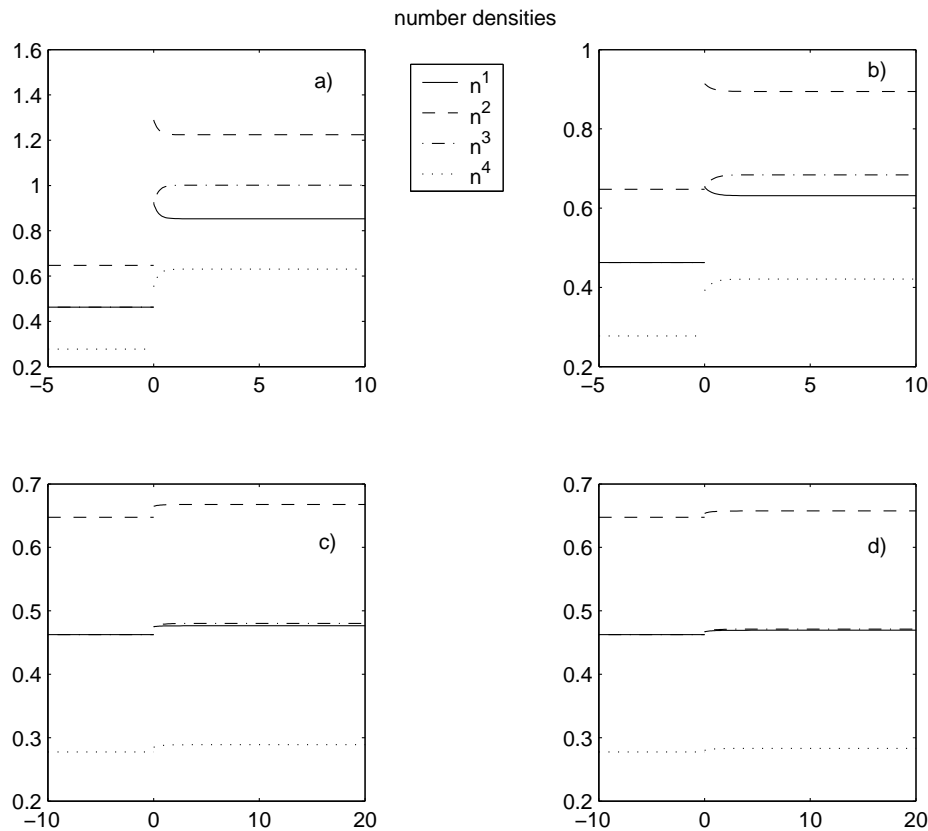


FIG. 5.8. Number densities versus x for the Mach numbers relevant to the four options a), b), c) d) (Problem C).

- [10] V. Giovangigli, *Multicomponent Flow Modeling*, Birkhäuser, Boston, 1999.
- [11] M. Groppi, P. Lichtenberger, F. Schürer and G. Spiga, *Conservative approximation schemes of kinetic equations for chemical reactions*, *Europ. J. Mech./B Fluids*, 27, 202–217, 2008.
- [12] M. Groppi and M. Pennacchio, *An IMEX finite volume scheme for reactive euler equations arising from kinetic theory*, *Commun. Math. Sci.*, 1, 449–470, 2003.
- [13] M. Groppi and G. Spiga, *Kinetic approach to chemical reactions and inelastic transitions in a rarefied gas*, *J. Math. Chem.*, 26, 197–219, 1999.
- [14] M. Groppi and G. Spiga, *A Bhatnagar–Gross–Krook–type approach for chemically reacting gas mixtures*, *Phys. of Fluids*, 16, 4273–4284, 2004.
- [15] M. Groppi, G. Spiga and S. Takata, *The steady shock problem in reactive gas mixtures*, *Bullet. Inst. Math. Acad. Sinica (New Series)*, 2, 935–956, 2007.
- [16] S. Kosuge, K. Aoki and S. Takata, *Shock-wave structure for a binary gas mixture: finite-difference analysis of the Boltzmann equation for hard-sphere molecules*, *Europ. J. Mech./B Fluids*, 20, 87–126, 2001.
- [17] G.M. Kremer, M. Pandolfi Bianchi and A.J. Soares, *A relaxation kinetic model for transport phenomena in a reactive flow*, *Phys. of Fluids*, 18(3), 037104–15, 2006.
- [18] I. Prigogine and E. Xhrouet, *On the perturbation of Maxwell distribution function by chemical reaction in gases*, *Physica*, XV, 913–932, 1949.
- [19] A. Rossani and A.M. Scarfone, *Travelling waves in a mixture of gases with bimolecular reversible reactions*, *Physica B*, 348, 198–205, 2004.
- [20] A. Rossani and G. Spiga, *A note on the kinetic theory of chemically reacting gases*, *Physica A*, 272, 563–573, 1999.

- [21] T. Ruggeri, *Global existence, stability and non linear wave propagation in binary mixtures of Euler fluids*, in *New trends in mathematical physics*, World Sci. Publ., Singapore, 205–214, 2004.
- [22] Y. Sone, *Kinetic Theory and Fluid Dynamics*, Birkhäuser Verlag, Boston, 2002.
- [23] W.G. Vincenti and C.H. Kruger, *Introduction to Physical Gas Dynamics*, Wiley, New York, 1965.
- [24] Ya.B. Zel'dovich and Yu.P. Raizer, *Physics of Shock Waves and High-Temperature Hydrodynamic Phenomena*, Dover, New York, 2002.